

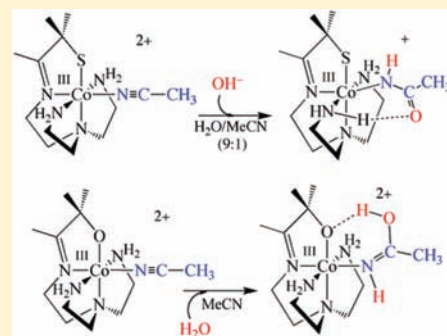
Nitrile Hydration by Thiolate- and Alkoxide-Ligated Co-NHase Analogues. Isolation of Co(III)-Amidate and Co(III)-Iminol Intermediates

Rodney D. Swartz, Michael K. Coggins, Werner Kaminsky,^S and Julie A. Kovacs*

The Department of Chemistry, University of Washington, Box 351700, Seattle, Washington 98195-1700, United States

S Supporting Information

ABSTRACT: Nitrile hydratases (NHases) are thiolate-ligated Fe(III)- or Co(III)-containing enzymes, which convert nitriles to the corresponding amide under mild conditions. Proposed NHase mechanisms involve M(III)-NCR, M(III)-OH, M(III)-imino, and M(III)-amide intermediates. There have been no reported crystallographically characterized examples of these key intermediates. Spectroscopic and kinetic data support the involvement of a M(III)-NCR intermediate. A H-bonding network facilitates this enzymatic reaction. Herein we describe two biomimetic Co(III)-NHase analogues that hydrate MeCN, and four crystallographically characterized NHase intermediate analogues, $[\text{Co}^{\text{III}}(\text{S}^{\text{Me}_2}\text{N}_4(\text{tren}))(\text{MeCN})]^{2+}$ (**1**), $[\text{Co}^{\text{III}}(\text{S}^{\text{Me}_2}\text{N}_4(\text{tren}))(\text{OH})]^{2+}$ (**3**), $[\text{Co}^{\text{III}}(\text{S}^{\text{Me}_2}\text{N}_4(\text{tren}))(\text{NHC}(\text{O})\text{CH}_3)]^{2+}$ (**2**), and $[\text{Co}^{\text{III}}(\text{O}^{\text{Me}_2}\text{N}_4(\text{tren}))(\text{NHC}(\text{O})\text{CH}_3)]^{2+}$ (**5**). Imino-bound **5** represents the first example of a Co(III)-imino compound in any ligand environment. Kinetic parameters ($k_1(298\text{ K}) = 2.98(5)\text{ M}^{-1}\text{ s}^{-1}$, $\Delta H^\ddagger = 12.65(3)\text{ kcal/mol}$, $\Delta S^\ddagger = -14(7)\text{ e.u.}$) for nitrile hydration by **1** are reported, and the activation energy $E_a = 13.2\text{ kcal/mol}$ is compared with that ($E_a = 5.5\text{ kcal/mol}$) of the NHase enzyme. A mechanism involving initial exchange of the bound MeCN for OH^- is ruled out by the fact that nitrile exchange from **1** ($k_{\text{ex}}(300\text{ K}) = 7.3(1) \times 10^{-3}\text{ s}^{-1}$) is 2 orders of magnitude slower than nitrile hydration, and that hydroxide bound **3** does not promote nitrile hydration. Reactivity of an analogue that incorporates an alkoxide as a mimic of the highly conserved NHase serine residue shows that this moiety facilitates nitrile hydration under milder conditions. Hydrogen-bonding to the alkoxide stabilizes a Co(III)-imino intermediate. Comparison of the thiolate versus alkoxide intermediate structures shows that $\text{C}\equiv\text{N}$ bond activation and $\text{C}=\text{O}$ bond formation proceed further along the reaction coordinate when a thiolate is incorporated into the coordination sphere.



INTRODUCTION

Nonenzymatic hydrolysis of nitriles by metal ions has been observed for most of the transition elements,¹ with the most efficient catalysts being Cu(II)² and Pt(II)³ complexes. Cobalt(III) complexes, however, tend to be poor catalysts, showing little or no catalytic turnover.^{4,5} This lack of turnover is likely a result of the substitution inert character of low-spin Co(III). For example, the rate at which $[\text{Co}^{\text{III}}(\text{NH}_3)_5(\text{H}_2\text{O})]^{3+}$ exchanges H_2O (at 298 K) is extremely slow ($k_{\text{off}} = 5.7 \times 10^{-6}\text{ s}^{-1}$).⁶ Despite this, nature incorporates a low-spin Co(III) ion in the metalloenzymes nitrile hydratases (Co-NHases),^{7–12} and some of these, depending on the organism and substrate, have been shown to have a higher rate of turnover than the iron-containing Fe-NHases. The active sites of nitrile hydratases (NHases) consist of low-spin Co(III) or Fe(III) ligated by two carboxamido nitrogens and three cysteine sulfurs (Figure 1), two of which are post translationally modified, one to a sulfinate (SO_2^-), and the other to a sulfenic acid (SOH).^{13,14} By tying up the π -symmetry sulfur orbitals, oxygenation of the two modified thiolates creates a ligand-field that is more like that of a σ -donating nitrogen than a π -donating thiolate.¹⁵ The higher than expected turnover rate for low-spin Co(III) NHase has been attributed to the trans influence of the thiolate, as well as the thiolates's tendency to favor lower coordination numbers.^{16,17}

Nitriles are extremely resistant to hydrolysis.^{1,5,18} Lewis acidic metal ions significantly enhance hydroxide-induced hydrolysis rates ($\sim 1 \times 10^6$) relative to that of a free nitrile ($1.6 \times 10^{-6}\text{ M}^{-1}\text{ s}^{-1}$)^{19,20} by stabilizing the developing charge on the anionic imidate intermediate, and thereby lowering the activation barrier. By binding to a metal ion, the nitrile carbon is activated toward nucleophilic attack. However, in contrast to the mild pH 7.5 aqueous conditions of NHase-promoted nitrile hydration,^{11,21–23} transition-metal promoted nitrile hydration typically requires OH^- base.¹ Free MeCN hydrolysis requires much harsher conditions (elevated temperatures, and $\text{M}[\text{OH}^-]$ concentrations), and proceeds all the way to the acid and amine.¹⁸ Both the +3 oxidation state, and low spin-state of NHase help to promote nitrile hydrolysis, by increasing the metal ion Lewis acidity. Metal ion Lewis acidity depends on the metal ion charge to size ratio (z/r).²⁰ Low-spin metal ions are smaller than their high-spin counterparts, and thus more Lewis acidic. It has also been suggested that a highly conserved H-bonding network, involving a nearby Ser-OH and Tyr-OH, helps to readily facilitate ambient temperature H_2O -induced nitrile hydration with NHase.^{11,22} Mutants lacking the Tyr-OH were shown to be inactive, whereas those

Received: September 28, 2010

Published: February 25, 2011

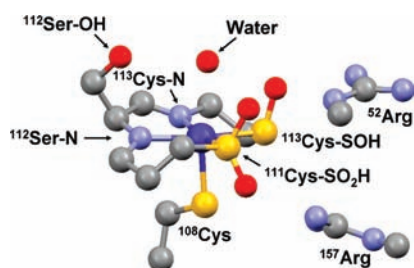


Figure 1. Co–NHase active site.

lacking the Ser–OH were shown to retain ~30% of the native activity.²⁴ Three distinct mechanisms of NHase-promoted nitrile hydrolysis have been proposed, two of which involve a catalytically active Co(III)–OH, and one that involves a Co(III)–NCR intermediate.^{11,14,20,22} Two of the three proposed mechanisms require the release of a Co(III)-bound product.²⁰ Spectroscopic²⁵ and kinetic^{11,22} data support the involvement of a M(III)-NCR, and there is significant literature precedent to support this mechanism,^{2,5,19,26,27} especially with transition-metals in the +3 oxidation state.²⁸

Examples of thiolate-ligated Fe- and Co-NHase models which hydrolyze nitriles are rare,^{29,30} and there are no examples in which amide- or iminol-ligated intermediates have been trapped. Kinetic parameters associated with the hydration of thiolate-ligated M(III)-NCR ($M = \text{Co}, \text{Fe}$) have yet to be reported. Such data could provide valuable insight into the mechanism of NHase-promoted hydration of nitriles to amides, as well as the role played by the metal ion versus the local protein environment.

Presented herein are the structure, properties, and kinetics of formation of a novel thiolate-ligated Co(III)-amidate complex that was obtained via hydroxide induced hydration of the corresponding thiolate-ligated Co(III)-NCMe complex. Reactivity is compared with a crystallographically characterized, thiolate-ligated Co(III)-OH complex. We also examine the reactivity of a derivative which incorporates a H-bonding alkoxide moiety as a mimic of the highly conserved NHase serine residue that, although not essential,²⁴ is proposed to facilitate nitrile hydration under mild pH 7.5 aqueous conditions.

EXPERIMENTAL SECTION

General Methods. All reactions were performed using standard Schlenk techniques under an atmosphere of dinitrogen. Reagents were obtained from Aldrich Chemical Co. and were used without further purification. Five-coordinate $[\text{Co}^{\text{II}}(\text{S}^{\text{Me}_2}\text{N}_4(\text{tren}))](\text{PF}_6)$ was synthesized as described elsewhere.³¹ Acetonitrile and diethyl ether were rigorously degassed and purified using solvent purification columns, housed in a custom stainless steel cabinet, and dispensed via a stainless steel Schlenk-line (GlassContour). Methanol (MeOH) was distilled from magnesium methoxide and degassed prior to use, and dichloromethane (DCM) was distilled from CaH_2 and degassed prior to use. NMR spectra were recorded on either a Bruker DPX 500 or AV 499 NMR spectrometer and referenced to the residual protio solvent. ^1H NMR chemical shifts (δ) are reported in parts per million (ppm) and coupling constants (J) are reported in Hz. ^{13}C NMR chemical shifts are reported in parts per million (ppm). IR spectra were obtained as KBr pellets and were recorded on a Perkin-Elmer 1700 FT-IR. Cyclic voltammograms were recorded in MeCN solutions with $\text{Bu}_4\text{N}(\text{PF}_6)$ (0.100 M) as the supporting electrolyte, using a EG&G Princeton Applied Research potentiostat with a glassy carbon working electrode, an SCE reference electrode, and a platinum auxiliary electrode. Electronic absorption spectra were recorded using either a Hewlett-Packard

8453 diode array or Cary 50 spectrometer. Elemental analyses were performed by Atlantic Microlab, Inc. (Norcross, GA).

Synthesis of $[\text{Co}^{\text{II}}(\text{S}^{\text{Me}_2}\text{N}_4(\text{tren}))](\text{MeCN})(\text{PF}_6)_2$ (1). Reduced $[\text{Co}^{\text{II}}(\text{S}^{\text{Me}_2}\text{N}_4(\text{tren}))](\text{PF}_6)$ (300 mg, 0.668 mmol) and $[\text{Cp}_2\text{Fe}](\text{PF}_6)$ (221 mg, 0.668 mmol) were dissolved in MeCN (200 mL) and allowed to stir overnight. The MeCN solution was evaporated to dryness and the remaining solid was washed with Et_2O and DCM until the washings were no longer colored. The solid was recrystallized from MeCN/ Et_2O to afford **1** as a green crystalline solid (260 mg, 0.409 mmol, 61.3% yield). Reduction potential (CH_3CN vs SCE): $E_p^{\text{a}} = -750$ mV. ^1H NMR (500 MHz, CD_3CN) δ 3.73 (t, $J = 7.1$ Hz, 2H), 3.63 (t, $J = 7.5$ Hz, 2H), 3.61–3.50 (m, 2H), 3.36 (dd, $J = 12.6, 4.6$ Hz, 2H), 3.32 (s, 2H), 3.25 (td, $J = 13.2, 7.4$ Hz, 2H), 3.12–2.98 (m, 2H), 2.77 (s, 2H), 2.14 (s, 3H), 1.53 (s, 6H). ^{13}C NMR (500 MHz, CD_3CN) δ ppm: 21.17, 33.04, 47.71, 57.21, 58.24, 59.40, 61.84, 133.83, 204.71. Electronic absorption spectrum (CH_3CN) λ_{max} (ϵ ($\text{M}^{-1} \text{cm}^{-1}$)): 295(12953), 450(402) nm. Elemental anal. Calcd for $\text{C}_{13}\text{H}_{28}\text{CoF}_{12}\text{N}_5\text{P}_2\text{S}$: C, 24.58; H, 4.44; N, 11.02. Found: C, 24.65; H, 4.42; N, 10.98. $\nu_{\text{C}\equiv\text{N}}$ 2328, 2302 cm^{-1} . $\nu_{\text{C}=\text{N}}$ 1628, 1597 cm^{-1} . ESI-MS m/z for $\text{C}_{11}\text{H}_{25}\text{CoN}_4\text{S}$: calcd, 304.1; found, 303.1.

Synthesis of $[\text{Co}^{\text{III}}(\text{S}^{\text{Me}_2}\text{N}_4(\text{tren}))(\text{NHC}(\text{O})\text{CH}_3)](\text{PF}_6)$ (2). A 1M MeOH solution of TBAOH (1.574 mL, 1.574 mmol) was slowly added to an MeCN (200 mL) solution of **1** (1 g, 1.574 mmol). The reaction was left to stir overnight, and then the solvent was evaporated to dryness. The resulting solid was washed with THF to remove $^n\text{Bu}_4\text{NPF}_6$ and recrystallized from MeCN/ Et_2O to afford **2** as a red crystalline solid. Electronic absorption spectrum (CH_3CN) λ_{max} (ϵ ($\text{M}^{-1} \text{cm}^{-1}$)): 368 (458), 500 (413). ^{13}C NMR (500 MHz, CD_3CN) δ ppm: 20.22, 28.76, 47.27, 56.15, 59.22, 60.68, 61.64, 185.02, 199.71. Elemental anal. Calcd for $\text{C}_{13}\text{H}_{29}\text{CoF}_{12}\text{N}_5\text{OPS}$: C, 30.77; H, 5.76; N, 13.80. Found: C, 29.50; H, 5.70; N, 11.83. $\nu_{\text{C}=\text{O}}$ 1576 cm^{-1} .

Synthesis of $[\text{Co}^{\text{III}}(\text{S}^{\text{Me}_2}\text{N}_4(\text{tren}))(\text{OH})](\text{PF}_6)$ (3). Reduced $[\text{Co}^{\text{II}}(\text{S}^{\text{Me}_2}\text{N}_4(\text{tren}))](\text{PF}_6)$ (100 mg, 0.223 mmol) and $[\text{Cp}_2\text{Fe}](\text{PF}_6)$ (74 mg, 0.223 mmol) were dissolved in “wet” MeOH. To this solution was added NaOMe (12 mg, 0.223 mmol) resulting in the formation of a red solution. The reaction was left to stir overnight. The solution was evaporated to dryness, washed with Et_2O , and recrystallized from MeCN/ Et_2O to afford **3** as a red crystalline solid.

Acetonitrile Exchange from $[\text{Co}^{\text{III}}(\text{S}^{\text{Me}_2}\text{N}_4(\text{tren}))(\text{MeCN})](\text{PF}_6)_2$ (1). $[\text{Co}^{\text{III}}(\text{S}^{\text{Me}_2}\text{N}_4(\text{tren}))(\text{MeCN})](\text{PF}_6)_2$ (**1**) (100 mg) was dissolved in CD_3CN (1 g) at -40 °C. The sample was then placed in an NMR probe that had been cooled to the desired temperature. The exchange of protio-acetonitrile for deuterio-acetonitrile was followed by ^{13}C NMR spectroscopy utilizing a 45° DEPT pulse sequence. A typical experiment involved collecting a spectrum every 30 min until the exchange was complete. The gem-dimethyl peak was used as a reference and the $\ln(\text{Integration}(\text{bound-MeCN})/\text{Integration}(\text{gem-dimethyls}))$ vs time was used to calculate the rate of k_{ex} .

Synthesis of $[\text{Co}^{\text{III}}(\text{O}^{\text{Me}_2}\text{N}_4(\text{tren}))(\text{MeCN})](\text{OTf})_2$ (4). Reduced $[\text{Co}^{\text{II}}(\text{O}^{\text{Me}_2}\text{N}_4(\text{tren}))](\text{OTf})$ was generated via a Schiff base condensation between *tris*(2-aminoethyl)amine (tren) (1.609 g, 11 mmol) and 3-methyl-3-hydroxy-2-butanone (1.123 g, 11 mmol) at a $\text{Co}^{\text{II}}\text{Cl}_2$ (1.298 g, 10 mmol) template in MeOH, followed by the addition of sodium trifluoromethanesulfonate (1.893 g, 10 mmol). This reaction mixture was allowed to stir overnight, the solvent was then evaporated to dryness, and the resulting solid was redissolved in a minimal amount of DCM, filtered through a Celite plug and recrystallized from a DCM/ Et_2O to afford $[\text{Co}^{\text{II}}(\text{O}^{\text{Me}_2}\text{N}_4(\text{tren}))](\text{OTf})$ as a green crystalline solid (1.136 g, 26% yield). Silver triflate (94 mg, 0.36 mmol) was then added to a 200 mL MeCN solution containing $[\text{Co}^{\text{II}}(\text{O}^{\text{Me}_2}\text{N}_4(\text{tren}))](\text{OTf})$ (160 mg, 0.36 mmol), and the reaction was allowed to stir overnight. Following this, the MeCN solvent was evaporated to dryness, and the remaining solid was washed with Et_2O . The solid was recrystallized from MeCN/ Et_2O to afford **4** as a green crystalline solid (130 mg, 54% yield). Reduction Potential (CH_3CN vs SCE): $E_p^{\text{c}} = -0.917$ V, $E_p^{\text{a}} = -1.01$ V. ^1H NMR (500 MHz, CD_3CN) δ 3.89 (t, $J = 7.3$ Hz, 4H),

3.55 (t, $J = 7.6$ Hz, 2H), 3.33 (s, 2H), 3.22 (tdd, $J = 25.9, 12.3, 5.3$ Hz, 4H), 3.11 – 2.95 (m, 4H), 2.18 (s, 3H), 1.25 (s, 6H). ^{13}C NMR (500 MHz, CD_3CN) δ ppm: 19.52, 30.01, 45.58, 53.04, 60.89, 62.50, 91.02, 120.68, 123.23, 125.39, 131.56, 206.48. $\nu_{\text{C}\equiv\text{N}}$ 2331, 2313 cm^{-1} . $\nu_{\text{C}=\text{N}}$ 1664, 1608 cm^{-1} . Electronic absorption spectrum (CH_3CN) λ_{max} (ϵ ($\text{M}^{-1} \text{cm}^{-1}$)): 371 (221). Elemental anal. Calcd for $\text{C}_{15}\text{H}_{28}\text{CoF}_6\text{N}_5\text{O}_7\text{S}_2$: C, 28.71; H, 4.50; N, 11.16. Found: C, 28.17; H, 4.53; N, 10.88.

Synthesis of $[\text{Co}^{\text{III}}(\text{O}^{\text{Me}2}\text{N}_4(\text{tren}))(\text{NHC}(\text{OH})\text{CH}_3)](\text{OTf})_2$ (5). Complex 4 (0.5 g, 1.518 mmol) was dissolved in an MeCN/ H_2O mixture and left to stir overnight. The reaction mixture was then evaporated to dryness, and the resulting solid was recrystallized from MeCN/ Et_2O to afford 5 as a red crystalline solid in quantitative yield. Reduction potential (CH_3CN vs SCE): $E_p^c = -151$ mV, $E_p^a = 42$ mV. Electronic absorption Spectrum (CH_3CN) λ_{max} (ϵ ($\text{M}^{-1} \text{cm}^{-1}$)): 350 (145), 478 (99), 547 (69) nm. $\nu_{\text{C}=\text{N}}$ 1685, 1664 cm^{-1} . ν_{OH} 3400 cm^{-1} . ν_{NH} 3325 cm^{-1} . Elemental anal. Calcd for $\text{C}_{15}\text{H}_{30}\text{CoF}_6\text{N}_5\text{O}_8\text{S}_2$: C, 27.91; H, 4.68; N, 10.85. Found: C, 27.85; H, 4.54; N, 10.72.

X-ray Crystallographic Structure Determination. A brown prism of 1 cut down to $0.24 \times 0.20 \times 0.19$ mm^3 was mounted on a glass capillary with oil. A brown plate of 2 ($0.46 \times 0.28 \times 0.28$ mm^3) and red prism of 3 ($0.30 \times 0.20 \times 0.12$ mm) were mounted on a glass capillary with oil. Brown cut-blocks of 4 ($0.59 \times 0.59 \times 0.23$ mm) and 5 ($0.24 \times 0.24 \times 0.59$ mm^3) were mounted on a glass capillary with oil. Data was collected at -143 °C on a Nonius Kappa CCD diffractometer. The crystal-to-detector distance was set to 30 mm for all five structures (1–5). The exposure time for 1 was 25 s per degree for all data sets, with a scan width of 1.4° . The exposure times for 2, 4, and 5 were 30 s per degree for all data sets, with a scan width of 1.0° . The exposure time for 3 was 120 s per degree for all data sets, with a scan width of 2.0° . Data collection for 1 was 91.9% complete to 28.30° and 98.5% complete to 25° in ϑ . Data collection for 2 was 86.1% complete to 29.65° in ϑ and 99.1% complete to 25° . Data collection for 3 was 96.7% complete to 24.47° in ϑ . Data collection for 4 was 86.8% complete to 29.79° in ϑ and 99.8% complete to 25° . Data collection for 5 was 85.7% complete to 29.94° in ϑ and 98.6% complete to 25° . A total of 56179 partial and complete reflections were collected for 1 covering the indices, $h = -10$ to 10, $k = -21$ to 21, $l = -24$ to 24. 5436 reflections were symmetry independent and the $R_{\text{int}} = 0.0965$ indicated that the data was of slightly less than average quality (average quality = 0.07). Indexing and unit-cell refinement indicated a monoclinic P lattice in the space group $P2_1/c$ (No. 14). A total of 49 099 partial and complete reflections were collected for 2 covering the indices, $h = -9$ to 9, $k = -20$ to 20, $l = -23$ to 23, 723 reflections were symmetry independent and the $R_{\text{int}} = 0.0687$ indicated that the data was of average quality (average quality = 0.07). Indexing and unit cell refinement indicated a monoclinic P lattice. The space group for 2 was found to be $P2_12_12_1$ (No. 19). A total of 69,442 partial and complete reflections were collected for 3 covering the indices, $h = -15$ to 15, $k = -10$ to 10, $l = -17$ to 14; 1538 reflections were symmetry independent and the $R_{\text{int}} = 0.0749$ indicated that the data was poor quality (0.07). Indexing and unit-cell refinement indicated an orthorhombic lattice. The space group for 3 was found to be $Pnma$ (No. 62). A total of 62 519 partial and complete reflections were collected for 4 covering the indices, $h = -11$ to 10, $k = -12$ to 13, $l = -26$ to 22; 11 331 reflections were symmetry independent and the $R_{\text{int}} = 0.0556$ indicated that the data was good quality (average quality = 0.07). Indexing and unit-cell refinement indicated a triclinic lattice. The space group for 4 was found to be $P1$ (No. 1). A total of 57 865 partial and complete reflections were collected for 5 covering the indices, $h = -12$ to 12, $k = -10$ to 10, $l = -44$ to 47; 6215 reflections were symmetry independent and the $R_{\text{int}} = 0.0573$ indicated that the data was good quality (0.07). Indexing and unit-cell refinement indicated a monoclinic lattice. The space group for 5 was found to be $P2_1/c$ (No. 14).

The data for 1–5 were integrated and scaled using hkl-SCALEPACK. The structure of complex 1 was solved by direct methods (DIRDIF)

producing a complete heavy atom phasing model consistent with the proposed structure. The structures of complexes 2–5 were solved by direct methods (SIR97) producing a complete heavy atom phasing model consistent with the proposed structure. For all five structures (1–5), all hydrogen atoms were located using a riding model. All non-hydrogen atoms were refined anisotropically by full-matrix least-squares. Crystal data for 1–5 are presented in Table 1. Selected bond distances and angles are compared in Table 2.

RESULTS AND DISCUSSION

Synthesis and Properties of Nitrile-Bound $[\text{Co}^{\text{III}}(\text{S}^{\text{Me}2}\text{N}_4(\text{tren}))(\text{NCCH}_3)](\text{PF}_6)_2$ (1) and its Hydrolyzed Deprotonated Acetamide Derivative $[\text{Co}^{\text{III}}(\text{S}^{\text{Me}2}\text{N}_4(\text{tren}))(\text{NHC}(\text{O})\text{CH}_3)]\text{PF}_6$ (2). Nitrile-bound 1 was synthesized via the addition of 1 equiv. of Cp_2FePF_6 to an acetonitrile solution of previously reported five-coordinate $[\text{Co}^{\text{II}}(\text{S}^{\text{Me}2}\text{N}_4(\text{tren}))](\text{PF}_6)$ (Scheme 1).³¹ The oxidized product was washed with diethyl ether and dichloromethane to remove the ferrocene and excess unreacted ferrocenium, and then recrystallized by layering diethyl ether onto an acetonitrile solution. This afforded 1 as a pure crystalline solid. The ^1H NMR of 1 (see Figure S1 in the Supporting Information) contains only peaks in the diamagnetic region consistent with a low-spin ($S = 0$) $\text{Co}(\text{III})$ ion. Peak assignments were made by running a HMQC experiment. Single crystals of 1 were grown via the slow diffusion of Et_2O into a MeCN solution of 1. Selected metrical parameters are listed in Table 2. As shown in the ORTEP diagram of Figure 2, $[\text{Co}^{\text{III}}(\text{S}^{\text{Me}2}\text{N}_4(\text{tren}))(\text{MeCN})]^{2+}$ (1) contains a coordinated MeCN cis to the thiolate sulfur and trans to the imine nitrogen (N(1)). The Co–S and Co–N bond distances of 1 are typical of low-spin $\text{Co}(\text{III})$ (mean Co–N bond length = 1.96 Å, mean Co–S bond length = 2.23 Å).³² Although the nitrile C≡N bond length (1.138(4) Å) of 1 is approximately the same (within error) as that of free acetonitrile (1.15(1) Å), the downfield shift to the ^{13}C NMR nitrile resonances ($\delta = 133.8$ and 5.30 ppm), relative to those of free acetonitrile (116.9 and 1.39 ppm), indicates that the nitrile carbon is more electrophilic in 1. This would suggest that the Lewis acidic metal ion activates the nitrile toward nucleophilic attack by polarizing the nitrile C≡N bond. Although the $\nu_{\text{C}\equiv\text{N}}$ stretch of 1 (2315 cm^{-1} vs $\nu_{\text{C}\equiv\text{N}}$ (free MeCN) = 2273 cm^{-1}) would suggest that the nitrile would be less susceptible to hydration, the observed facile conversion of nitrile-bound 1 to the corresponding amidate (vide infra) proves otherwise.

Titration of KOH (in 0.06 equiv aliquots) to an aqueous ($\text{H}_2\text{O}/\text{MeCN}$ (9:1)) solution of 1 (allowing 5 min for equilibration between each addition) results in the loss of the band at 450 (402) nm, and the formation of a new species, 2, with bands at 368 (458) nm and 500 (413) nm (Figure 3). One equivalent of KOH is required in order for the reaction to reach completion. No reaction is observed if H_2O , as opposed to OH^- , is added to 1.

Ambient temperature hydroxide addition also causes a noticeable change in the ^{13}C NMR (see Figure S3 in the Supporting Information), whereupon the peaks associated with bound acetonitrile ($\delta = 133.83$ and 5.30 ppm; see Figure S2 in the Supporting Information) disappear, and two new peaks ($\delta = 185.02, 28.76$ ppm) appear. The position of these new peaks relative to free acetamide (178.0 and 22.1 ppm) would be consistent with the formation of a bound acetamide. Single crystals of the product, $[\text{Co}^{\text{III}}(\text{S}^{\text{Me}2}\text{N}_4(\text{tren}))(\text{NHC}(\text{O})\text{CH}_3)](\text{PF}_6)$ (2), obtained via slow diffusion of Et_2O into an MeCN solution of 2 confirmed this. As shown by the ORTEP diagram of 2 (Figure 4), and number of counterions per cationic complex, the coordinated acetamide is deprotonated.

Table 1. Crystal Data, Intensity Collections^a, and Structure Refinement Parameters for [Co^{III}(S^{Me}₂N₄(tren))(MeCN)](PF₆)₂ (1), [Co^{III}(S^{Me}₂N₄(tren))(NHC(O)CH₃)](PF₆) (2), [Co^{III}(S^{Me}₂N₄(tren))(OH)](PF₆) (3), [Co^{III}(O^{Me}₂N₄(tren))(MeCN)](OTf)₂ (4), and [Co^{III}(O^{Me}₂N₄(tren))(NHC(OH)CH₃)](OTf)₂ (5)

	1	2	3	4	5
formula	C ₁₃ H ₂₈ Co F ₁₂ N ₅ P ₂ S	C ₁₃ H ₂₉ Co F ₆ N ₅ OPS	C ₁₁ H ₂₆ Co F ₆ N ₄ OPS	C ₃₆ H ₆₅ Co ₂ F ₁₂ N ₁₃ O ₁₄ S ₄	C ₁₅ H ₃₀ Co F ₆ N ₅ O ₈ S ₂
MW	635.33	507.38	466.33	1378.15	645.51
T, K	130(2) K	130(2) K	130(2) K	130(2) K	130(2)
unit cell	monoclinic	orthorhombic	orthorhombic	triclinic	monoclinic
a (Å)	8.0740(3)	7.5760(6)	13.4890(7)	8.4743(2)	8.5790(8)
b (Å)	16.1330(7)	14.5673(13)	8.7463(12)	9.9717(3)	8.356(2)
c (Å)	18.6270(8)	18.3780(18)	15.1258(13)	19.2114(6)	34.839(8)
α (deg)	90	90	90	92.846(2)	90
β (deg)	100.591(2)	90	90	94.772(2)	90.58(1)
γ (deg)	90	90	90	114.4133	90
V (Å ³)	2385.0(2)	2028.2(3)	1784.5(3)	1466.82(7)	2497.3(9)
Z	4	4	4	1	4
d(calcd) (g/cm ³)	1.769	1.662	1.736	1.560	1.717
space group	P2 ₁ /c	P2 ₁ 2 ₁ 2 ₁	Pnma	P1	P2 ₁ /c
R ^b	0.0507	0.0565	0.0749	0.0556	0.0510
R _w ^{c,d}	0.0891	0.1281	0.1731	0.1480	0.1263
GOF	1.001	1.073	1.055	1.092	1.040

^a Mo Kα (λ = 0.7107 Å) radiation; graphite monochromator; -90 °C. ^b R = Σ||F_o| - |F_c||/Σ|F_o|. ^c R_w = [Σw(|F_o| - |F_c||)²/ΣwF_o²]^{1/2}, where w⁻¹ = [σ²_{count} + (0.05F²)²]/4F². ^d R_w = {Σ[w(F_o² - F_c²)²]/Σ[w(F_o²)²]}^{1/2}; w = 1/[σ²(F_o²) + (0.00620P)² + 0.000P], where P = [F_o² + 2F_c²]/3.

Table 2. Selected Bond Distances (Å) and Bond Angles (deg) for Nitrile-Bound [Co^{III}(S^{Me}₂N₄(tren))(MeCN)](PF₆)₂ (1), Acetamidate-Bound [Co^{III}(S^{Me}₂N₄(tren))(NHC(O)CH₃)](PF₆) (2), Hydroxide-Bound [Co^{III}(S^{Me}₂N₄(tren))(OH)](PF₆) (3), Nitrile-Bound [Co^{III}(O^{Me}₂N₄(tren))(MeCN)](OTf)₂ (4), and Iminol-Bound [Co^{III}(O^{Me}₂N₄(tren))(NHC(OH)CH₃)](OTf)₂ (5)

	1	2	3	4	5
Co-X(1)	2.208(1)	2.209(1)	2.217(3)	1.858(5)	1.881(2)
Co-N(1)	1.875(2)	1.897(4)	1.892(8)	1.844(5)	1.866(2)
Co-N(2)	1.973(3)	1.980(4)	1.971(8)	1.953(4)	1.940(3)
Co-N(3)	1.963(3)	1.959(4)	1.935(6)	1.950(4)	1.961(2)
Co-N(4)	1.948(3)	1.963(4)	1.935(6)	1.965(4)	1.955(2)
Co-N(5)	1.917(3)	1.946(4)	N/A	1.929(5)	1.950(2)
Co-OH	N/A	N/A	1.869(6)	N/A	N/A
N(5)-C(12)	1.138(4)	1.323(7)	N/A	1.137(7)	1.261(4)
C(12)-O	N/A	1.267(6)	N/A	N/A	1.337(4)
N(1)-C(4)	1.271(4)	1.284(7)	1.280(11)	1.283(7)	1.277(4)
X(1)-Co-N(1)	86.23(9)	86.6(1)	86.2(2)	84.9(2)	83.0(1)
X(1)-Co-N(2)	174.27(9)	173.9(1)	174.3(2)	173.2(2)	171.0(1)
X(1)-Co-N(5)	90.44(9)	91.4(1)	N/A	91.0(2)	91.9(1)
X(1)-Co-OH	N/A	N/A	95.8(2)	N/A	N/A
Co-N(5)-C(12)	172.9(3)	135.6(4)	N/A	172.2(4)	128.9(2)
N(3)-Co-N(4)	170.1(1)	170.6(2)	170.7(3)	171.4(2)	171.4(1)
N(3)-Co-N(5)	88.9(1)	90.4(2)	N/A	87.3(2)	89.5(1)
N(4)-Co-N(5)	87.6(1)	87.2(2)	N/A	89.9(2)	87.2(2)
N(3)-Co-OH	N/A	N/A	87.7(2)	N/A	N/A
N(1)-Co-N(5)	176.7(1)	177.8(2)	N/A	175.8(2)	174.9(1)
N(1)-Co-OH	N/A	N/A	178.0(3)	N/A	N/A

X = S, O *N(4) = N(3') for this structure, since a crystallographic mirror plane relates the two atoms N(3) and N(3').

Selected bond lengths for [Co^{III}(S^{Me}₂N₄(tren))(NHC(O)CH₃)](PF₆) (2) are listed in Table 2. Comparison of the structural data for nitrile-bound 1 and acetamidate-bound 2 reveals that the metal ion coordination sphere remains relatively unchanged upon hydration, with the notable exceptions being the lengthening of the Co-N(5) (1.917(3) Å to 1.946(4) Å) and Co-N(1) (1.875(2) Å to 1.897(4) Å) bonds (Table 2). The latter is likely a result of the

strong *trans* influence of the anionic amidate,³³ and the former is likely due to the conversion of N(5) from sp to sp² hybridization. Based on its Co(III)-N(5) bond length (1.946(4) Å), the amidate appears to be more weakly bound to 2 relative to, for example, [Co^{III}(NH₃)₅(NHC(O)CH₃)]²⁺ (Co-N(amidate) = 1.911 Å),³³ possibly due to the incorporation of an anionic thiolate in the coordination sphere. The amidate C=O(1) oxygen is weakly H-bonded to the primary amine N(3)-H proton (N(3)-H...O(1) = 1.90 Å; N(3)...O(1) = 2.71 Å; N(3)-H-O(1) = 145.5°), thereby locking it into a position that is orthogonal to the CoS(1)N(1)N(2)N(5) plane. Acetamidate-ligated 2 represents the first example of an intermediate-bound NHase analogue. Examples of structurally analogous pairs of Co(III)-nitrile and Co(III)-amidate complexes are rare.

In contrast to nitrile-bound [Co^{III}(S^{Me}₂N₄(tren))(MeCN)]²⁺ (1), crystallized samples of its hydroxide-bound derivative, [Co^{III}(S^{Me}₂N₄(tren))(OH)](PF₆) (3; Figure 5), does not appear to promote MeCN hydration, as monitored by UV/vis electronic absorption spectroscopy. Acetamide is not detected (by ¹H NMR or GC/MS) in reactions between 3 and MeCN, even upon heating in neat MeCN. A diamagnetic ¹H NMR, and significantly shorter Co-S (2.217(3) Å) and Co-N (mean = 1.933 Å) bond lengths in 3 relative to our reduced five-coordinate [Co^{II}(S^{Me}₂N₄(tren))] derivative³¹ (Co-S = 2.297(1) Å; mean Co-N = 2.111 Å), provide evidence that 3 is a low-spin (S = 0) Co(III)-OH, as opposed to an S = 3/2 or S = 1/2 Co(II)-OH₂. Although reactivity of our Co(III)-OH, 3, contrasts with Mascharak's observations,^{29,34} these results suggest that a Co(III)-NCR intermediate is more likely to be involved in NHase-promoted nitrile hydrolysis. This would be consistent with recent kinetic data.¹¹

Kinetics of [Co^{III}(S^{Me}₂N₄(tren))(MeCN)]²⁺ (1)-Promoted Nitrile Hydration. To understand the mechanism of nitrile hydrolysis by 1, the kinetics of this reaction were monitored at low temperature (0 °C) using electronic absorption spectroscopy. All reactions were run under pseudo-first-order conditions with at least a 10-fold excess concentration of OH⁻, and a fixed concentration of Co(III)-MeCN (limiting reagent). The concentration of hydroxide (OH⁻), was allowed to vary from 11 to 55 mM. Nonlinear fits (see Figure S4 in the Supporting

Scheme 1

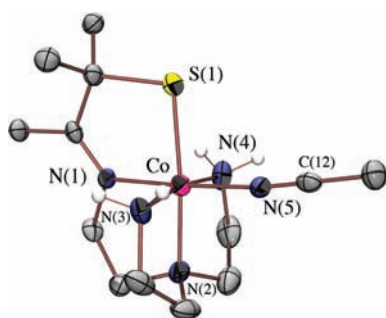
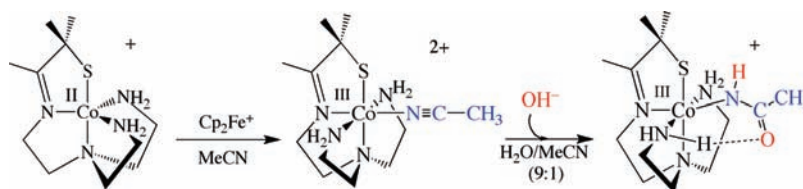


Figure 2. ORTEP of $[\text{Co}^{\text{III}}(\text{S}^{\text{Me}_2}\text{N}_4(\text{tren}))(\text{MeCN})]^{2+}$ (1) showing 50% probability ellipsoids and the atom labeling scheme. With the exception of the primary amines, all other hydrogens have been omitted for clarity.

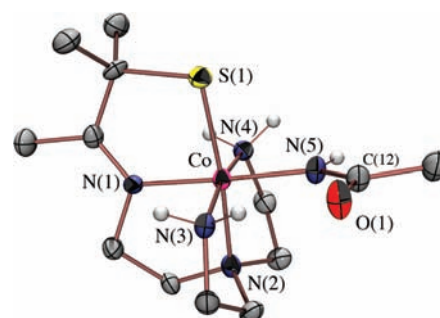


Figure 4. ORTEP of $[\text{Co}^{\text{III}}(\text{S}^{\text{Me}_2}\text{N}_4(\text{tren}))(\text{NHC}(\text{O})\text{CH}_3)]^+$ (2) showing 50% probability ellipsoids and the atom labeling scheme. With the exception of the primary amine and acetamido hydrogens, all other hydrogens have been omitted for clarity.

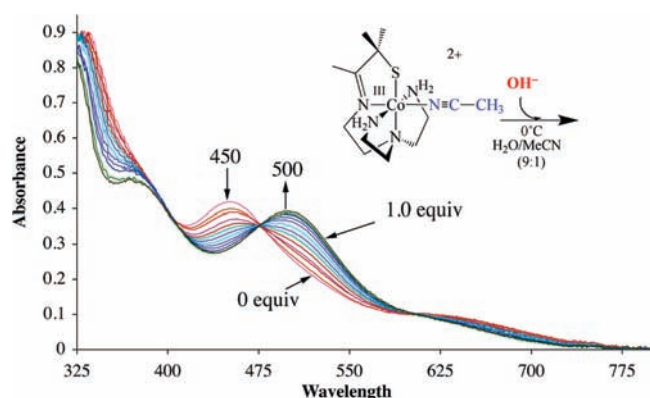


Figure 3. Monitoring the hydration reaction between $[\text{Co}^{\text{III}}(\text{S}^{\text{Me}_2}\text{N}_4(\text{tren}))(\text{MeCN})]^{2+}$ (1) and KOH in $\text{H}_2\text{O}/\text{MeCN}$ (9:1) at 273 K by electronic absorption spectroscopy, showing that 1 equiv. of KOH is required for the reaction to reach completion.

Information), to the first-order eq 1, using global analysis over the entire wavelength range (and a

$$A_t = A_\infty + (A_0 - A_\infty)e^{-kt} \quad (1)$$

program written for MATLAB), afforded the pseudo first-order rate constants, k_{obs} , shown in Figure 7, indicating that the reaction is first-order in **1** ($\text{Co}^{\text{III}}\text{NCMe}$; eq 2). A representative absorbance versus time plot showing a nonlinear fit (pink) to the experimental data (blue) is shown in Figure 6. The observed pseudo first-order rate

$$\text{Rate} = k_1[\text{Co}^{\text{III}}\text{NCMe}][\text{OH}^-] \quad (2)$$

$$k_{\text{obs}} = k_1[\text{OH}^-] \quad (3)$$

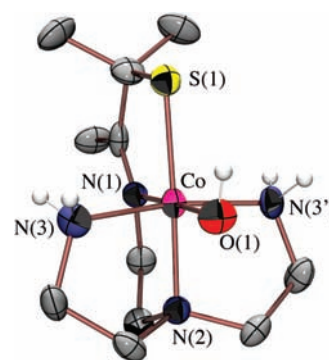


Figure 5. ORTEP of $[\text{Co}^{\text{III}}(\text{S}^{\text{Me}_2}\text{N}_4(\text{tren}))(\text{OH})](\text{PF}_6)$ (3) showing 50% probability ellipsoids and the atom labeling scheme. With the exception of the amine and hydroxide hydrogens, all other hydrogens have been omitted for clarity.

constant, k_{obs} , was obtained at several KOH concentrations, and the second-order rate constant $k_1(273 \text{ K}) = 0.70(5) \text{ M}^{-1}\text{s}^{-1}$, which relates to k_{obs} according to eq 3, was obtained from the slope of a k_{obs} vs $[\text{OH}^-]$ plot (Figure 7). The slope of the $\log(k_{\text{obs}})$ vs $\log([\text{OH}^-])$ plot (0.92; see Figure S5 in the Supporting Information) indicates that the reaction is first-order with respect to hydroxide. Activation parameters for the conversion of nitrile-bound **1** to acetamido-bound **2** ($\Delta H^\ddagger = 12.65(3) \text{ kcal/mol}$, $\Delta S^\ddagger = -14(7) \text{ e.u.}$) were obtained by determining k_1 at several different temperatures, and examining an Eyring plot ($\ln(k_1/T)$ vs $1/T$) (Figure 8). The activation parameters were then used to calculate the ambient temperature second order rate constant, $k_1(298 \text{ K}) = 2.98(5) \text{ M}^{-1}\text{s}^{-1}$, for I-promoted hydration of MeCN. This rate constant is comparable to that for nitrile hydration by $[\text{Co}^{\text{III}}(\text{NH}_3)_5(\text{H}_2\text{O})]^{3+}$ ($3.40 \text{ M}^{-1}\text{s}^{-1}$),¹⁹ 6 orders of magnitude greater than for hydration of free MeCN,¹⁹ and 3 orders of magnitude faster than the intramolecular

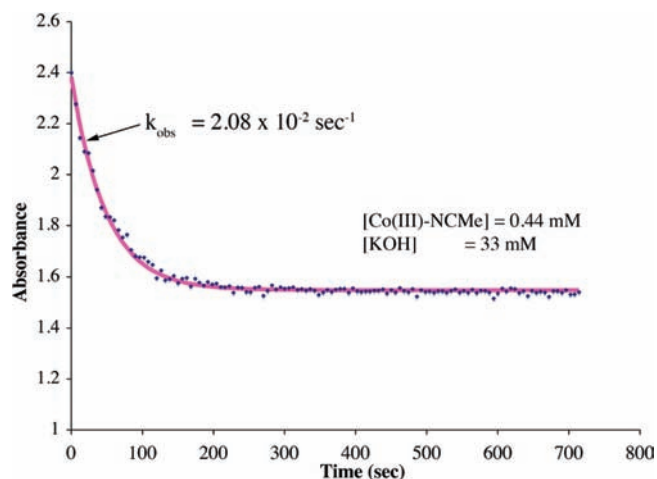


Figure 6. Calculated nonlinear fit (pink) to the experimental data (blue) for the reaction between $[\text{Co}^{\text{III}}(\text{S}^{\text{Me}_2}\text{N}_4(\text{tren}))(\text{MeCN})](\text{PF}_6)_2$ (**1**) and KOH in $\text{H}_2\text{O}/\text{MeCN}$ (9:1) at 273 K to afford amidate-bound $[\text{Co}^{\text{III}}(\text{S}^{\text{Me}_2}\text{N}_4(\text{tren}))(\text{NHC}(\text{O})\text{CH}_3)](\text{PF}_6)$ (**2**).

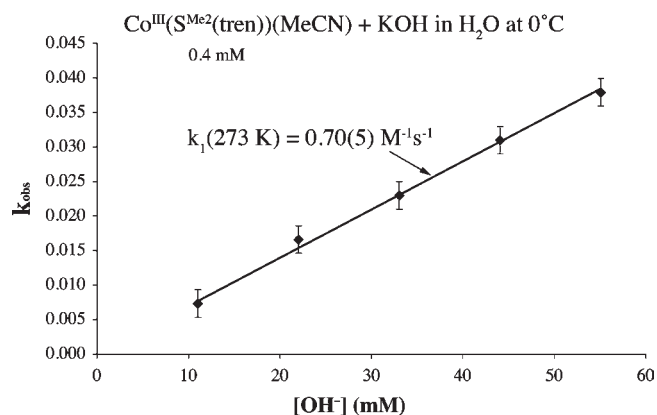


Figure 7. k_{obs} vs $[\text{OH}^-]$ plot for the reaction between 0.4 mM $[\text{Co}^{\text{III}}(\text{S}^{\text{Me}_2}\text{N}_4(\text{tren}))(\text{MeCN})](\text{PF}_6)_2$ (**1**) and KOH in $\text{H}_2\text{O}/\text{MeCN}$ (9:1) at 273 K under pseudo-first-order conditions (with excess (11–55 mM) KOH), showing the second-order rate constant k_1 , which is obtained from the slope.

cis-OH^- -promoted hydration of $[(\text{cyclen})\text{Co}(\text{III})(\text{MeCN})\text{-(OH)}]^{2+}$ ($k_2 = 4.7 \times 10^{-3} \text{ s}^{-1}$).⁵ Cobalt nitrile hydratase (Co-NHase) catalyzes the hydration of benzonitrile significantly faster with a k_{cat}/K_m of $6.5(1) \times 10^3 \text{ mM}^{-1} \text{ s}^{-1}$.¹¹ The activation energy for **1**-promoted hydration of coordinated MeCN (with ~ 10 mM KOH), $E_a = 13.2 \text{ kcal/mol}$ (55.2 kJ/mol), was determined from an Arrhenius plot (see Figure S6 in the Supporting Information). This is significantly larger than that of NHase ($E_a = 5.5 \text{ kcal/mol}$ (23(1) kJ/mol),¹¹ but significantly lower than that ($E_a = 20.3 \text{ kcal/mol}$) of free MeCN (with 0.65 M OH^-).¹⁸

The kinetic data for **1**-promoted nitrile hydration is consistent with a mechanism (Scheme 2) involving rate-determining attack of hydroxide at a coordinated nitrile carbon step to afford an (unobserved) iminol intermediate (**I**), which then rapidly tautomerizes to the deprotonated amidate **2**. An iminol intermediate is proposed to form in NHase-promoted nitrile hydrolysis.¹¹

An alternative mechanism would involve initial exchange of the coordinated acetonitrile for hydroxide, which then subsequently reacts with free acetonitrile to afford an oxygen-bound iminol species,

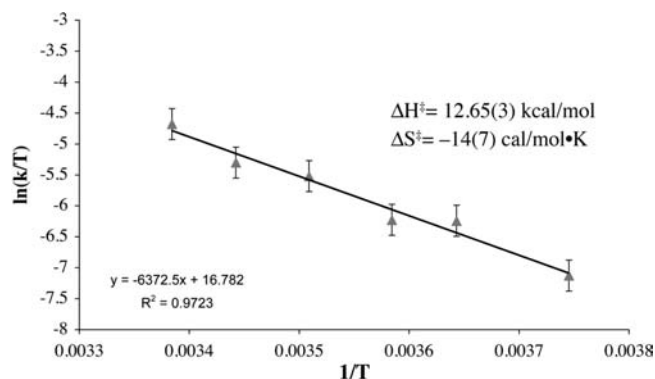
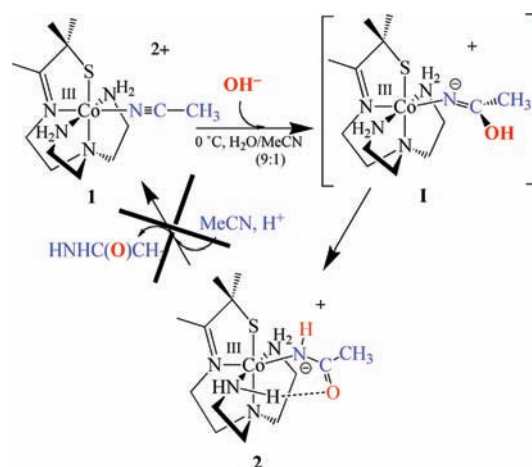


Figure 8. Eyring plot for the variable temperature reaction between $[\text{Co}^{\text{III}}(\text{S}^{\text{Me}_2}\text{N}_4(\text{tren}))(\text{MeCN})](\text{PF}_6)_2$ (**1**) and KOH in $\text{H}_2\text{O}/\text{MeCN}$ (9:1) to afford acetamidate-bound $[\text{Co}^{\text{III}}(\text{S}^{\text{Me}_2}\text{N}_4(\text{tren}))(\text{NHC}(\text{O})\text{CH}_3)](\text{PF}_6)$ (**2**).

Scheme 2



which then rearranges to the observed nitrogen-bound acetamidate complex **2**. This mechanism would, however, require an additional $\text{Co}(\text{III})\text{-L}$ bond cleaving step with a system that is typically substitution inert. In contrast to *trans*-cysteinate-ligated NHase, *cis*-thiolate ligated $[\text{Co}^{\text{III}}(\text{S}^{\text{Me}_2}\text{N}_4(\text{tren}))(\text{NHC}(\text{O})\text{CH}_3)]^+$ (**2**) does not release the amide product, thereby preventing turnover (Scheme 2). The anionic nature of the amidate may be in part responsible for tight binding of product to our model. However, even in the presence of a proton donor ($\text{NH}_4^+\text{PF}_6^-$), acetamide release is not observed. It is also possible that the intramolecular H-bond between the ligand's primary amine N–H proton and the amidate carbonyl oxygen is, in part, responsible for tight acetamidate binding. However, based on the $\text{N}(3)\text{-H}\cdots\text{O}(1)$, and $\text{N}(3)\cdots\text{O}(1)$ distances (Figure 4, vide supra), this H-bond appears to be rather weak. Another possibility is that the substitution inert nature of the low-spin $\text{Co}(\text{III})$ ion, and the absence of a *trans* thiolate, is responsible. Dissociation of the coordinated acetamide during the $[(\text{cyclen})\text{Co}(\text{III})(\text{MeCN})\text{-(OH)}]^{2+}$ promoted catalytic hydration of MeCN, for example, is slow ($k_{\text{diss}} = 3.3 \times 10^{-4} \text{ s}^{-1}$).^{4,5} Previously we showed that *trans* thiolates can increase k_{ex} rates for low-spin $\text{Co}(\text{III})$ by as much as 4 orders of magnitude, even for anionic ligands ($k_{\text{ex}}([\text{Co}^{\text{III}}(\text{NH}_3)_5\text{-(H}_2\text{O})]^{3+}) = 5.8 \times 10^{-6} \text{ s}^{-1}$ vs $k_{\text{ex}}([\text{cis,trans-Co}^{\text{III}}(\text{S}_2^{\text{Me}_2}\text{N}_3(\text{Pr, Pr}))(\text{N}_3)] = 2.1(5) \times 10^{-2} \text{ s}^{-1}$). To rule out the possibility that the

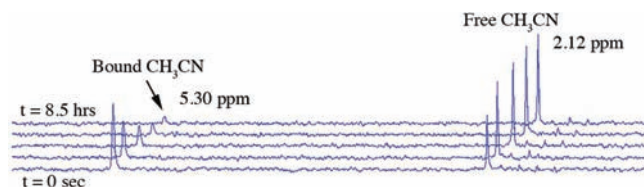


Figure 9. Time versus ^{13}C NMR CH_3 peak intensity stack plot monitoring the exchange of bound CH_3CN for CD_3CN .

mechanism of nitrile hydration by **1** involves the initial exchange of acetonitrile for hydroxide, and in order to determine how the *cis* versus *trans* positioning of the thiolate ligand influences ligand exchange, we examined the kinetics of nitrile exchange from **1**.

Acetonitrile Exchange Rate. Acetonitrile was found to bind reversibly to **1**. In the presence of one equivalent of CD_3CN , the ^{13}C NMR spectrum of **1** (Figure 9) is characterized by the presence of four signals corresponding to the methyl and nitrile carbons of both bound and free acetonitrile (bound 133.8 $\text{C}\equiv\text{N}$, 5.30 CH_3 ; free 118.7 $\text{C}\equiv\text{N}$, 2.12 CH_3 (ppm)). The fact that the resonances for bound and free acetonitrile are well-resolved peaks indicates that the nitrile exchange rate must be slower than $1 \times 10^1 \text{ s}^{-1}$ at 300 K,³⁵ and that exchange rates could be monitored by ^{13}C NMR. The rate constant, k_{ex} for acetonitrile exchange was determined by following the disappearance of the bound $-\text{CH}_3\text{CN}$ methyl peak (5.30 ppm) over time as it was replaced by CD_3CN (Figure 10). Nonlinear fits to the first-order eq 4 (where I_0 , I_{∞} , and I_t are the initial, final, and absolute integration of the peak at 5.30 ppm at time t , respectively)

$$I_t = I_{\infty} + (I_0 - I_{\infty})e^{-kt} \quad (4)$$

showed that the data are consistent with a first-order process, and afforded the exchange rate constants, k_{ex} shown in Table 3. Activation parameters ($\Delta H^\ddagger = 10.7(7)$ kcal/mol and $\Delta S^\ddagger = -32(6)$ e.u.) were determined by obtaining k_{ex} at several temperatures (Table 3), and examining an Eyring ($\ln(k_{\text{ex}}/T)$ vs $1/T$) plot (see Figure S7 in the Supporting Information). Calculation of k_{ex} at 300 K gives an ambient temperature rate constant of $7.3(1) \times 10^{-3} \text{ s}^{-1}$ for nitrile exchange from $[\text{Co}^{\text{III}}(\text{S}^{\text{Me}_2}\text{N}_4(\text{tren}))(\text{MeCN})]^{2+}$ (**1**). The fact that k_{ex} (300 K) is more than 2 orders of magnitude slower than nitrile hydration ($k_1(298 \text{ K}) = 2.98(5) \text{ M}^{-1} \text{ s}^{-1}$), rules out a mechanism involving a $\text{Co}(\text{III})-\text{OH}$ which forms via the exchange of MeCN for OH^- . Also, given that $[\text{Co}^{\text{III}}(\text{S}^{\text{Me}_2}\text{N}_4(\text{tren}))(\text{OH})](\text{PF}_6)_3$ (**3**; Figure 5) does not appear to react with MeCN (vide supra), provides further evidence to suggest that the reactive species is unlikely to be a metal-bound hydroxide. Nitrile exchange from **1** is slightly slower than azide exchange from low-spin, *trans*-thiolate ligated $[\text{Co}^{\text{III}}(\text{S}_2\text{Me}_2\text{N}_3(\text{Pr},\text{Pr})(\text{N}_3))] (k_{\text{off}} = 2.1(5) \times 10^{-2} \text{ s}^{-1})$,¹⁶ but 3 orders of magnitude faster than water exchange from $[\text{Co}^{\text{III}}(\text{NH}_3)_5(\text{H}_2\text{O})]^{3+}$ ($k_{\text{off}} = 5.7 \times 10^{-6} \text{ s}^{-1}$).⁶ So, even though it is *cis*, as opposed to *trans* to the nitrile, the anionic thiolate does appear to contribute to an enhancement of exchange rates, a property that would be critical to promoting product release, and thus catalytic turnover.

Influence of Sulfur on Nitrile Hydration. To see how the thiolate influences the nitrile hydration reaction mechanism involving **1**, we synthesized the alkoxide derivative and examined its reactivity. An added benefit of incorporating an alkoxide moiety, is that it provides a mimic of the highly conserved NHase serine residue that, although not essential,²⁴ is proposed to facilitate nitrile hydration under milder pH = 7.5 aqueous conditions.^{11,22} Alkoxide-ligated $[\text{Co}^{\text{II}}(\text{O}^{\text{Me}_2}\text{N}_4(\text{tren}))](\text{OTf})$ was synthesized in situ via a metal ion templated Schiff base condensation between 3-methyl-3-hydroxy-

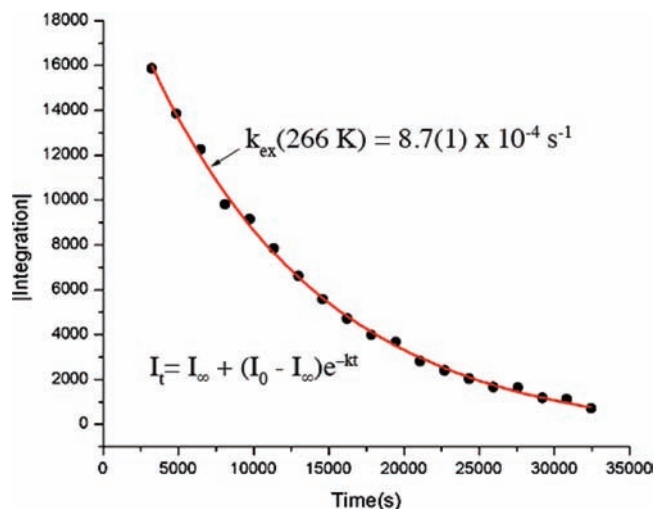


Figure 10. Calculated nonlinear fit (red) to the experimental data (•••) for CH_3CN exchange from $[\text{Co}^{\text{III}}(\text{S}^{\text{Me}_2}\text{N}_4(\text{tren}))(\text{MeCN})]^{2+}$ (**1**) in CD_3CN as monitored by the integrated ^{13}C NMR CH_3 peak intensity over time.

Table 3. Temperature-Dependent Rate Constants, k_{off} for Nitrile Release from $[\text{Co}^{\text{III}}(\text{S}^{\text{Me}_2}\text{N}_4(\text{tren}))(\text{MeCN})](\text{PF}_6)_2$ (**1**)

T (K)	k_{ex} (s^{-1})
228.3	$2.34(8) \times 10^{-5}$
244.7	$1.01(4) \times 10^{-4}$
261.0	$4.25(5) \times 10^{-4}$
266.4	$8.7(1) \times 10^{-4}$

butanone and *tris*(2-aminoethyl)amine (tren), and then oxidized, via the addition of AgOTf in acetonitrile, to afford nitrile-bound $[\text{Co}^{\text{III}}(\text{O}^{\text{Me}_2}\text{N}_4(\text{tren}))(\text{MeCN})](\text{OTf})_2$ (**4**). Complex **4** is air-stable in the solid state. However, solutions of **4** exhibit hydrolysis, even in the presence of trace amounts of water. The presence of a bound nitrile was verified by X-ray crystallography. Selected bond lengths are contained in Table 2. As shown in the ORTEP diagram of Figure 11, MeCN binds *trans* to the imine nitrogen N(1), and *cis* to the alkoxide oxygen O(1).

As was the case with thiolate-ligated **1**, the nitrile $\text{C}\equiv\text{N}$ bond is slightly shortened relative to free acetonitrile (1.137 Å for **4** vs 1.15 Å for free MeCN). The higher-frequency $\nu_{\text{C}\equiv\text{N}}$ stretch 2321 cm^{-1} associated with **4**, relative to that of free MeCN (2273 cm^{-1}) indicates that the metal ion of **4** polarizes the $\text{C}\equiv\text{N}$ bond, making the nitrile carbon more electrophilic. The position of the nitrile carbon resonance in the ^{13}C NMR ($\delta = 131.5$), as well as the reactivity of **4** is consistent with this.

In contrast to thiolate-ligated $[\text{Co}^{\text{III}}(\text{S}^{\text{Me}_2}\text{N}_4(\text{tren}))(\text{MeCN})](\text{PF}_6)_2$ (**1**), which requires hydroxide (KOH_{aq} ($\sim 10 \text{ mM}$)) to hydrolyze the coordinated nitrile, the nitrile of alkoxide-ligated $[\text{Co}^{\text{III}}(\text{O}^{\text{Me}_2}\text{N}_4(\text{tren}))(\text{MeCN})]^{2+}$ (**4**) can be hydrolyzed with neutral water. Addition of 4000 equiv of H_2O to an acetonitrile solution of **4** (1:20 v/v) causes the band at 371 nm in the electronic absorption spectrum to disappear, and new bands at 350, 478, and 547(sh) nm to grow in (Figure 12). Crystalline samples of the product of this reaction, $[\text{Co}^{\text{III}}(\text{O}^{\text{Me}_2}\text{N}_4(\text{tren}))(\text{NHC}(\text{OH})\text{CH}_3)](\text{OTf})_2$ (**5**), were obtained via Et_2O diffusion into an MeCN solution of **8**. The ORTEP diagram of Figure 13, and bond lengths of Table 2, show that nitrile hydration of alkoxide-ligated **4** affords a $\text{Co}(\text{III})$ -bound iminol (Scheme 3), in contrast to the hydration

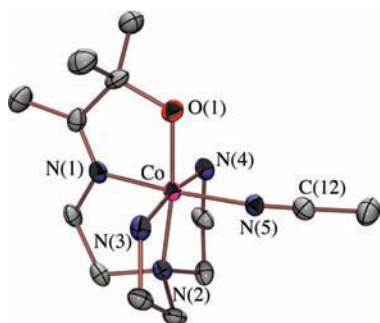


Figure 11. ORTEP of $[\text{Co}^{\text{III}}(\text{O}^{\text{Me}_2\text{N}_4(\text{tren}))}(\text{MeCN})]^{2+}$ (**4**) showing 50% probability ellipsoids and the atom labeling scheme. Hydrogens have been omitted for clarity.

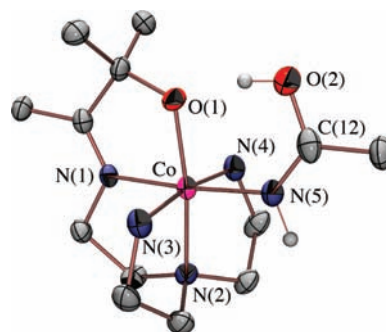


Figure 13. ORTEP of $[\text{Co}^{\text{III}}(\text{O}^{\text{Me}_2\text{N}_4(\text{tren}))}(\text{NHC}(\text{OH})\text{CH}_3)]^{2+}$ (**5**) showing 50% probability ellipsoids and the atom labeling scheme. Hydrogens have been omitted for clarity.

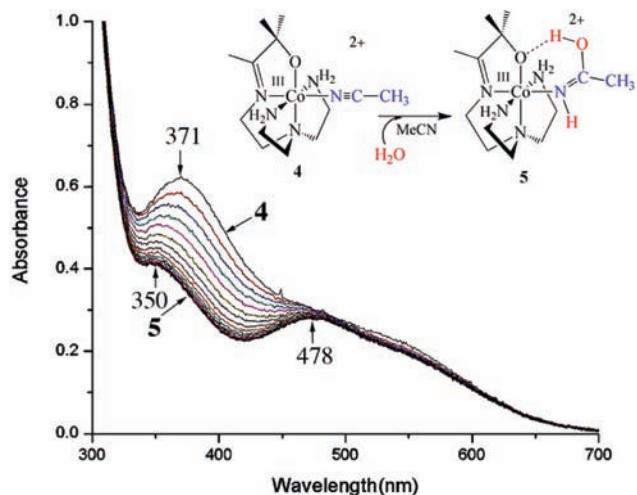
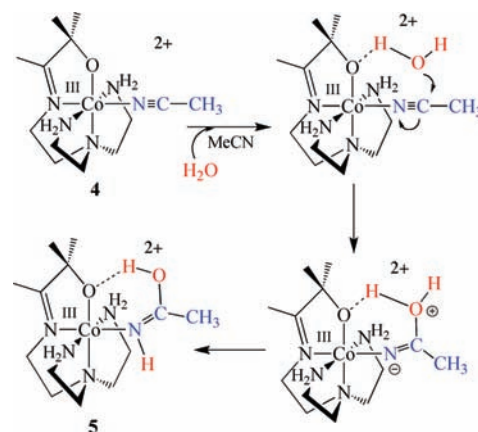


Figure 12. Monitoring the hydration reaction between $[\text{Co}^{\text{III}}(\text{O}^{\text{Me}_2\text{N}_4(\text{tren}))}(\text{MeCN})]^{2+}$ (**4**) and H_2O (4000 equiv.) by electronic absorption spectroscopy over the course of 2 h at ambient temperature.

reaction of thiolate-ligated **1**, which affords a Co(III)-bound acetamidate (Figure 4, Scheme 2). With free acetamide, on the other hand, the acetamide tautomeric form is adopted almost exclusively ($K_{\text{eq}} = 1 \times 10^8$) over the iminol tautomeric form.^{36,37} Transition-metal iminol species are rather rare, and only a few structures have been reported, involving Ni, Ru, or Pt.^{38–41} The hydrated C(12)–N(5) bond in thiolate-ligated **2** (1.323(7) Å) is significantly longer than in alkoxide ligated **5** (1.261(4) Å) consistent with a more activated C–N bond in **2** (relative to **5**). Both C(12)–N(5) bonds are significantly longer than the corresponding nitrile complex (1.137(7) Å in **1**; 1.138(4) Å in **4**). In **5**, this bond is significantly shorter than that of free acetamide (1.333 Å),⁴² slightly shorter than the imine C(4)=N(1) bonds of **1–5** (Table 2), and closer to that of a C=N double (1.28 Å)⁴³ as opposed to C–N single (1.47 Å)⁴³ bond, consistent with an imine alcohol (iminol) formulation (Scheme 3). The C(12)–O bond is considerably shorter in thiolate-ligated **2** (1.267(6) Å), relative to alkoxide-ligated **5** (1.337(4) Å), showing that C–O bond formation has proceeded further along the reaction coordinate in **2** (see Figure S8 in the Supporting Information). In **5**, this bond lies closer to that of a single C–O (1.41 Å)⁴³ than that of a double C=O (1.20 Å)⁴³ bond. In **2**, this bond is close to that of free acetamide (1.233 Å).⁴² Whereas, the C(12)–O(2) and C(12)–N(5) bond lengths in **5** (Table 2) both differ significantly from previously reported Co(III)–acetamide

Scheme 3



structures, including $[\text{Co}^{\text{III}}(\text{NH}_3)_5(\text{NHCOCH}_3)]^{2+}$ (C–O = 1.267(12) Å; C–N = 1.339(12) Å),³³ and $(\text{cyclen})\text{Co}^{\text{III}}(\eta^2\text{-N}(\text{H})\text{C}(\text{O})\text{Me})$ (C–O = 1.28(1) Å; C–N = 1.32(1) Å).⁵ Bond distances within the iminol moiety of **5** (Table 2) lie closer to that expected for alcohol/imine structure, even when compared with one of few previously reported transition-metal iminol complexes, $(R,S,R,S)\text{-}[\text{Ni}(\text{L})(\text{NHC}(\text{OH})\text{CH}_3)]^+$ (C–O = 1.242(7) Å; C–N = 1.314(7) Å; L = 1,3,6,8,12,15-hexaazatricyclo[13.3.1.18,12]-icosane).⁴⁰ An O-bound linkage isomer for iminol **5** is ruled out by an increase in R-value during refinement of the X-ray structure. Although transition-metal iminol compounds are rare,^{38–41} the N-bound linkage isomer (observed in **5**) tends to be the thermodynamically favored form.³⁶

The orientation of the iminol N(5)C(12)O(2) plane in **5** (Figure 11) is orthogonal to that of the amidate in **2** (Figure 4). These orthogonal orientations optimize H-bonding interactions between the alkoxide oxygen, and ligand's primary amine N–H proton, for **5** and **2**, respectively. Rotation of the acetamidate moiety to a plane that is roughly perpendicular to that of the thiolate containing S(1)Co(N(1)N(2)N(5)) also minimizes steric interactions between S(1) and O(1). The longer Co–O(1) alkoxide and C(12)–O(2) bonds in **5** (1.881(2) Å) relative to **4** (1.858(5) Å), and unusually short O(1)···O(2) separation (2.400 Å) provide evidence to support the presence of a proton on O(2) in **5**. The iminol O(1)···H distance, and O(1)···H–O(2) angle is 1.589 Å and 161.3°, respectively. H-bonds are weaker in the amidate structure, with a N(4)–H···O(1) distance of 1.895 Å and a

N(4)···O(1) separation of 2.699 Å. The N(4)–H–O(1) angle is 144.7°.

As described above, a comparison of bond lengths in thiolate and alkoxide structures **2** and **5** shows that nitrile C≡N bond cleavage has proceeded further along the reaction coordinate (Scheme 3, see Figure S8 in the Supporting Information) in the thiolate-ligated complex. Hydration stops at the Co(III)–iminol with the alkoxide complex (Scheme 3), but proceeds further to the Co(III)–amidate in the thiolate complex (see Figure S8 in the Supporting Information). A Co(III)–iminol intermediate is proposed to form during the NHase catalytic cycle, although this has yet to be observed.^{11,22} There are two reasonable explanations for the observed differences in reactivity for thiolate- and alkoxide-ligated nitrile complexes **1** and **4**. First, the metal ion in alkoxide-ligated **4** is presumably more Lewis acidic than in **1**, given the electron withdrawing capabilities of an alkoxide relative to a thiolate. Previously we showed that thiolates decrease metal ion Lewis acidity relative to alkoxides.¹⁷ The more Lewis acidic metal ion of **4** would facilitate hydration under milder conditions with a weaker nucleophile (H₂O vs OH[−]). Second, if the alkoxide H-bonds to the incoming water molecule (Scheme 3), then the water would become more nucleophilic as a result. A highly conserved Ser-OH residue is proposed to play a similar role in NHase.^{11,22} In the case of our synthetic model, **5**, H-bonding to the alkoxide (to form a 6-membered chelate ring; Scheme 3) would then stabilize the iminol tautomer (protonated at the oxygen), and prevent its rearrangement to the corresponding amide (protonated at the nitrogen), by locking the proton into position and inhibiting its transfer to the nitrogen. The proton on the oxygen would favor the resonance structure containing a single as opposed to double C–O bond. Given the lower propensity of thiolates to H-bond, this intermediate would be less stable when the alkoxide is replaced with a thiolate, thus favoring rearrangement of the iminol intermediate to an amidate. Hydroxide-induced hydration would initially afford a deprotonated iminol (missing the proton at the nitrogen; see Figure S8 in the Supporting Information). As long as the iminol OH proton is not locked into position via a H-bond, then coordination to the Co(III) ion, via the nitrogen, would favor rearrangement of this deprotonated iminol to the amidate by stabilizing negative charge build-up at the nitrogen (see Figure S8 in the Supporting Information). Proton transfer from either the doubly protonated iminol oxygen intermediate preceding **5** (Scheme 3), or the singly protonated iminol oxygen intermediate preceding **2** (see Figure S8 in the Supporting Information), to the nitrogen could either be intramolecular, or assisted by water. With NHase, proton transfer is believed to be mediated by a highly conserved H-bonding network.^{11,22}

SUMMARY AND CONCLUSIONS

In summary, a biomimetic Co–NHase analogue is described which binds both MeCN and OH[−] to afford NHase intermediate analogues, [Co^{III}(S^{Me2}N₄(tren))(MeCN)]²⁺ (**1**) and [Co^{III}-(S^{Me2}N₄(tren))(OH)]⁺ (**3**), both of which were crystallographically characterized. The nitrile of low-spin (*S* = 0) **1** is activated toward nucleophilic attack by OH[−] (~10 mM), and nitrile hydration occurs readily (*k*₁(298 K) = 2.98(5) M^{−1} s^{−1}, Δ*H*[‡] = 12.65(3) kcal/mol, Δ*S*[‡] = −14(7) e.u.) to afford acetamidate-ligated [Co^{III}-(S^{Me2}N₄(tren))(NHC(O)CH₃)]⁺ (**2**). Thiolate-ligated **2** is the first reported example of a NHase Co(III)–amide intermediate analogue. The activation energy of this hydration reaction (*E*_a = 13.2

kcal/mol) is significantly lower than that (*E*_a = 20.3 kcal/mol) of free MeCN (with 0.65 M OH[−]),¹⁸ but higher than that (*E*_a = 5.5 kcal/mol) of the NHase enzyme,¹¹ most likely because **1** lacks the conserved H-bonding network which facilitates enzymatic nitrile hydration. A mechanism involving initial exchange of the bound MeCN for OH[−] is ruled out by the fact that nitrile exchange from **1** (*k*_{ex}(300 K) = 7.3(1) × 10^{−3} s^{−1}) is 2 orders of magnitude slower than nitrile hydration. The fact that hydroxide bound **3** does not promote nitrile hydration also rules out this mechanism. In contrast to *trans* cysteine-ligated Co–NHase, **2** does not release the amide product (even in the presence of a proton donor), thereby preventing turnover. A likely reason for this is that the cationic charge of **2** increases product affinity. The penta-anionic ligand environment of the NHase Co(III) ion, and *trans* stabilizing effect of the thiolate, prevents this problem with NHase. When an alkoxide is incorporated in place of the thiolate of **1**, in [Co^{III}(O^{Me2}N₄(tren))(MeCN)]²⁺ (**4**), nitrile hydration is facilitated under milder conditions (with H₂O as opposed to OH[−]) to afford a rare example of a crystallographically characterized iminol-bound intermediate [Co^{III}(O^{Me2}N₄(tren))(NHC(OH)CH₃)]²⁺ (**5**). This is the first reported example of a Co(III)–iminol. With **4**, this reaction is so facile that even residual water in acetonitrile can lead to hydrolysis. The alkoxide mimics the conserved NHase serine, which is proposed to promote nitrile hydration by H-bonding to the incoming H₂O and facilitating proton exchange. H-bonding to the alkoxide in **5** stabilizes the iminol tautomeric form. Comparison of the bond lengths in hydrated nitrile intermediates of thiolate-ligated **2** versus alkoxide-ligated **5**, shows that the thiolate causes C≡N bond activation, and C=O bond formation to proceed further along the reaction coordinate. The thiolate's decreased propensity to H-bond prevents the reaction from stopping at the iminol—a proposed, yet unobserved, NHase intermediate.

ASSOCIATED CONTENT

S Supporting Information. Contains crystallographic data for complexes **1–5**, HMQC (¹H, ¹³C), and ¹³C NMR spectra of **1**, and a ¹³C NMR spectrum of **2**. Kinetics data, including Eyring and Arrhenius plots for the hydration of **1** and **4**. And a proposed mechanism for Co(III)–MeCN conversion to Co(III)–(NHC(O)CH₃). This material is available free of charge via the Internet at <http://pubs.acs.org>.

AUTHOR INFORMATION

Corresponding Author

kovacs@chem.washington.edu

Author Contributions

[§]UW staff crystallographer.

ACKNOWLEDGMENT

Funding from the NIH (RO1 GM 45881) is gratefully acknowledged.

REFERENCES

- (1) Kukulshkin, V. Y.; Pombeiro, A. J. L. *Inorg. Chim. Acta* **2005**, *358*, 1–21.
- (2) Breslow, R.; Fairweather, R.; Keana, J. J. *Am. Chem. Soc.* **1967**, *89*, 2135–2138.
- (3) Jensen, C. M.; Troglor, W. C. *J. Am. Chem. Soc.* **1986**, *108*, 723–729.

- (4) Chin, J.; Kim, J. H. *Angew. Chem., Int. Ed.* **1990**, *29*, 523–525.
- (5) Kim, J. H.; Britten, J.; Chin, J. *J. Am. Chem. Soc.* **1993**, *115*, 3618–3622.
- (6) Gonzalez, G.; Moullet, B.; Martinez, M.; Merbach, A. E. *Inorg. Chem.* **1994**, *33*, 2330.
- (7) Miyanaga, A.; Fushinobu, S.; Ito, K.; Wakagi, T. *Biochem. Biophys. Res. Commun.* **2001**, *288*, 1169–1174.
- (8) Payne, M. S.; Wu, S.; Fallon, R. D.; Tudor, G.; Stieglitz, B.; Turner, I. M. J.; Nelson, M. J. *Biochemistry* **1997**, *36*, 5447–5454.
- (9) Brennan, B. A.; Alms, G.; Scarrow, R. C. *J. Am. Chem. Soc.* **1996**, *118*, 9194–9195.
- (10) Kobayashi, M.; Nishiyama, M.; Nagasawa, T.; Horinouchi, S.; Beppu, T.; Yamada, H. *Biochim. Biophys. Acta* **1991**, *1129*, 23–33.
- (11) Mitra, S.; Holz, R. C. *J. Biol. Chem.* **2007**, *282*, 7397–7404.
- (12) Nojiri, M.; Nakayama, H.; Odaka, M.; Yohda, M.; Takio, K.; Endo, I. *FEBS Lett.* **2000**, *465*, 173–177.
- (13) Nagashima, S.; Nakasako, M.; Naoshi, D.; Tsujimura, M.; Takio, K.; Odaka, M.; Yohda, M.; Kamiya, N.; Endo, I. *Nat. Struct. Biol.* **1998**, *5*, 347–351.
- (14) Huang, W.; Jia, J.; Cummings, J.; Nelson, M.; Schneider, G.; Lindqvist, Y. *Structure* **1997**, *5*, 691–699.
- (15) Lugo-Mas, P.; Dey, A.; Xu, L.; Davin, S. D.; Benedict, J.; Kaminsky, W.; Hodgson, K. O.; Hedman, B.; Solomon, E. I.; Kovacs, J. A. *J. Am. Chem. Soc.* **2006**, *128*, 11211–11221.
- (16) Shearer, J.; Kung, I. Y.; Lovell, S.; Kaminsky, W.; Kovacs, J. A. *J. Am. Chem. Soc.* **2001**, *123*, 463–468.
- (17) Brines, L. M.; Villar-Acevedo, G.; Kitagawa, T.; Swartz, R. D.; Lugo-Mas, P.; Kaminsky, W.; Benedict, J. B.; Kovacs, J. A. *Inorg. Chim. Acta* **2008**, *361*, 1070–1078.
- (18) Rabinovitch, B. S.; Winkler, C. A. *Can. J. Research* **1949**, *20B*, 185–188.
- (19) Buckingham, D. A.; Keene, F. R.; Sargeson, A. M. *J. Am. Chem. Soc.* **1973**, *17*, 5649–5652.
- (20) Kovacs, J. A. *Chem. Rev.* **2004**, *104*, 825–848.
- (21) Kobayashi, M.; Shimizu, S. *Nat. Biotechnol.* **1998**, *16*, 733–736.
- (22) Rao, S.; Holz, R. C. *Biochemistry* **2008**, *47*, 12057–12064.
- (23) Kobayashi, M.; Nagasawa, T.; Yamada, H. *Tibtech* **1992**, *10*, 402–408.
- (24) Yamanaka, Y.; Hashimoto, K.; Ohtaki, A.; Noguchi, K.; Yohda, M.; Odaka, M. *J. Biol. Inorg. Chem.* **2010**, *15*, 655–665.
- (25) Sugiura, Y.; Kuwahara, J.; Nagasawa, T.; Yamada, H. *J. Am. Chem. Soc.* **1987**, *109*, 5848–5850.
- (26) Kukushkin, V. Y.; Pombeiro, A. J. L. *Chem. Rev.* **2002**, *102*, 1771–1802.
- (27) Balahura, R. J.; Cock, P.; Purcell, W. L. *J. Am. Chem. Soc.* **1974**, *96*, 2739–2742.
- (28) Zanella, A. W.; Ford, P. C. *Inorg. Chem.* **1975**, *14*, 42–47.
- (29) Noveron, J. C.; Olmstead, M. M.; Mascharak, P. K. *J. Am. Chem. Soc.* **1999**, *121*, 3553–3554.
- (30) Heinrich, L.; Mary-Verla, A.; Li, Y.; Vaissermann, J.; Chottard, J. C. *Eur. J. Inorg. Chem.* **2001**, 2203–2206.
- (31) Brines, L. M.; Shearer, J.; Fender, J. K.; Schweitzer, D.; Shoner, S. C.; Barnhart, D.; Kaminsky, W.; Lovell, S.; Kovacs, J. A. *Inorg. Chem.* **2007**, *46*, 9267–9277.
- (32) Based on a survey of the Cambridge Crystallographic Database.
- (33) Schneider, M.; Ferguson, G.; Balahura, R. *Can. J. Chem.* **1973**, *51*, 2180.
- (34) Noveron, J. C.; Olmstead, M. M.; Mascharak, P. K. *J. Am. Chem. Soc.* **2001**, *123*, 3247–3259.
- (35) Drago, R. S. *Physical Methods for Chemists*; 2nd ed.; Saunders: Orlando, FL, 1992.
- (36) Fairlie, D. P.; Woon, T. C.; Wickramasinghe, W. A.; Willis, A. C. *Inorg. Chem.* **1994**, *33*, 6425–6428.
- (37) Sigel, H.; Martin, R. B. *Chem. Rev.* **1982**, *82*, 385.
- (38) Nagao, H.; Hirano, T.; Tsuboya, N.; Shiota, S.; Mukaida, M.; Oi, T.; Yamasaki, M. *Inorg. Chem.* **2002**, *41*, 6267–6273.
- (39) Cini, R.; Fanizzi, F. P.; Intini, F. P.; Maresca, L.; Natile, G. *J. Am. Chem. Soc.* **1993**, *115*, 5123–5131.
- (40) Suh, M. P.; Oh, K. Y.; Lee, J. W.; Bae, Y. Y. *J. Am. Chem. Soc.* **1996**, *118*, 777–783.
- (41) Cini, R.; Fanizzi, F. P.; Intini, F. P.; Natile, G. *J. Am. Chem. Soc.* **1991**, *113*, 7805–7806.
- (42) Zobel, D.; Luger, P.; Dreissig, W.; Koritsanszky, T. *Acta Crystallogr., Sect. B* **1992**, *48*, 837.
- (43) March, J. *Advanced Organic Chemistry*; John Wiley and Sons: New York, 1985.